JMGCB
ISSN:3032-1085
https://doi.org/10.61796/jmgcb.v1i7.747

ANTIBIOFILM SILVER NANOPARTICLES PRODUC BY ESCHERICHIA COLI

Mohammed aqeel abdulrazz
Department of Biology, College of Education, Qurna University of Basrah, Basrah, IRAQ

Ismaal Jmia Abas
Department of Biology, College of Education, Qurna University of Basrah, Basrah, IRAQ
m7703d@gmail.com

Received: May 22, 2024; Accepted: Jun 10, 2024; Published: Jul 17, 2024;

Abstract: E. coli bacteria were obtained from the soil near the Euphrates River in the northern region of Basra City and cultured on nutrient agar media. The bacterial isolate was subjected to purification and thereafter seen under a microscope. The study revealed that E. coli bacteria has the capacity to synthesize silver nanoparticles when combined with a 1 mM AgNO3 solution. The synthesis of AgNPs was deduced by examining the change in color of the reaction mixture. The UV-vis spectroscopy results indicated that the silver nanoparticles exhibited absorbance at a specific wavelength of 428 nm. Additionally, the FT-IR analysis revealed the presence of active groups in the silver particles, which played a role in maintaining their stability. The SEM and TEM studies revealed that the AgNPs exhibited a spherical morphology, with diameters ranging from 47.66 to 11.68 nm. A cubic crystal structure of silver was confirmed using an X-ray diffraction examination, while an EDX test indicated that the final product was silver (Ag). The antimicrobial efficacy of silver nanoparticles (AgNPs) against bacteria isolated from diseased patients was evaluated using the Well diffusion agar technique. It was shown that nano-silver effectively inhibited the development of the bacteria.The study utilized 96 well Microtiter plates to assess the inhibitory effect of AgNPs on biofilm development in harmful bacteria.

Keywords: Biosynthesis of silver nanoparticles, inhibition of biofilm, XRD, EDX, , E. coli and 96 well microtiter plate

Introduction

The extracellular synthesis method was used in the synthesis of silver nanoparticles from E. coli bacteria because this method is less expensive, has high productivity, and has a high percentage of purity. In general, the method of biosynthesis using living organisms is considered to have an advantage over physical and chemical methods because these methods require The use of highly toxic materials to reduce silver nitrate salts to silver nanoparticles requires energy consumption and advanced equipment [1]. E. coli bacteria were used in the synthesis of silver nanoparticles because they possess reducing factor that contributed to reducing AgNO3 to AgNPs [2]. The nanoparticles were characterized by many characteristics and features that distinguished them from other materials, as many techniques and devices were used to describe them, as SEM explained. And TEM showed that the diameters of the nanoparticles ranged from 1 to 100 nm, and the nanoparticles were

characterized by their absorbance at wavelengths (420 to 470 nm) when using UV-visible spectroscopy. The active groups attached to the nanoparticles contributed to the stability and stabilization of the particles when detected by the FT-IR device. The silver nanoparticles have a cubic crystalline structure that distinguishes them from the rest of the materials when using the Nanoparticles possessed unique biological properties in addition to their structural rigidity despite their atomic structure, high tolerance to high temperatures, the ability to conduct electricity, and their large surface area compared to Its size is [3]. Recently, the widespread use of antibiotics has led to a decrease in their ability to kill pathogenic bacteria such as Pseudomonas aeruginosa, E. coli, Klebsiella pneumonia, and Staphylococcus aureus, so it was necessary to carry out medical interventions to reduce this risk [4]. The defense mechanisms found in disease-causing bacterial species are efflux pumps and biofilms. The biofilm plays an important role in antibiotic resistance, as it gives the bacteria inside the biofilm a thousand times more resistance than those bacteria that are free and floating [5]. In addition to the importance of the biofilm in retaining water and nutrients in harsh environmental conditions [6], Silver nanoparticles had the ability to penetrate the biofilm and adhere to the bacterial cell membrane. The small size of the silver nanoparticles enabled them to pass through the biofilm , which leads to changes in the composition of the plasma membrane of the bacterial cell and leads to the collapse of the membrane and thus leakage of cell contents and death. Cell [7].

Methods

2-1: Collecting samples

The soil was dug up to a depth of 5 cm. The soil sample was taken from the edge of the river, kept in a sterile plastic bottle, and transported to the laboratory. 1 gram of soil was weighed and dissolved in 5 ml of distilled water and mixed with a vortex, and a cotton swab was used to spread the suspension. on a Petri dish containing the nutrient agar medium [8].

2-2: Diagnosis of bacterial isolates

The study utilized the cultural characteristics of E. coli bacteria when grown on nutrient agar medium and MacConky agar medium, as well as their phenotypic characteristics when stained with the Gram stain and observed under a microscope to determine the shape and arrangement of the cells. Additionally, biochemical tests were conducted, and a molecular diagnostic examination was performed using PCR with 16SrRNA and DNA size detection by comparing it with a ladder through gelelectrophoresis [9].

2–3: Prepare a solution of silver nitrate.

A solution of silver nitrate (AgNO3) was prepared at a concentration of 1 mM by dissolving 42.1 mg in 100 ml of distilled water and stored in a tightly closed, opaque glass box to avoid oxidation until used [10].

2-4: Biosynthesis of silver nanoparticles

An E. coli bacterial culture was prepared by inoculating isolates of the bacteria into a 250-ml conical flask containing 100 ml of nutrient broth medium. The flask was then placed in a shaking incubator set at a temperature of 37 °C and a rotation speed of 150 rpm for 24 hours. Following the completion of the incubation time, the bacterial culture was subjected to centrifugation at a speed of 8000 revolutions per minute in order to gather the liquid portion (supernatant) in a glass container. A total of 90 ml of the liquid portion of the E. coli bacteria was combined with 10 ml of a solution containing silver nitrate. The resulting combination was then placed in a shaking incubator and kept at a temperature of 37 °C for a duration of 24 hours, with the rotation speed set at 150 rpm. Following the completion of the incubation period, the reaction mixture underwent a color change, which serves as the initial sign of the formation of silver nanoparticles [11].

2-5: Characterization of silver nanoparticles

2-5-1: Change in color

The change in color of the reaction mixture is the first indication of the formation of silver nanoparticles as a result of the reduction of silver nitrate salts to silver nanoparticles, $Ag^{+} \rightarrow Ag^{0}$ [12].

2-5-2: UV-visible spectroscopy

A UV-visible spectrophotometer device with a wavelength of 200–1000 nm) was used to detect the absorbance of the silver nanoparticles. The supernatant solution was used to zero the device, and the absorbance of the silver nanoparticles was measured, as the silver nanoparticles have a wavelength ranging between 420 and 470 nm. [13].

2-5-3: Fourier transform infrared (FT- IR) spectroscopy

Powdered silver nanoparticles resulting from biosynthesis were used with potassium bromide tablets and examined with an FT-IR device to detect the active groups, which contributed to the stability of the nanoparticles [14].

2-5-4: Scanning electron microscope (SEM) and Transmission electron microscope (TEM).

SEM and TEM were used to detect the sizes of the silver nanoparticles formed, to clarify their shape, and to know the nature of the AgNPs surface by sending a beam of focused electrons with high precision for the purpose of obtaining a microscopic image of the silver nanoparticles while verifying the homogeneity of the examined material [15].

2-5-5 : X-ray diffraction (XRD)

A X-ray diffraction (XRD) instrument was employed to ascertain the crystalline and structural properties of the synthesized silver nanoparticles. The experiment utilized a Shimadzu 600 device equipped with a monochromatic copper beam of 0.15406 nm wavelength. The device operated at a power of 4 kilovolts and a current of 30 amps. The scanning speed was set at 6.02 degrees within an angular range of 2Θ. The ray entry hole had a diameter of 0.3 mm. The experiment involved placing powdered silver nanoparticles on the surface of a silicon slice in the XRD device [16].

2-5-6 : Energy diffraction X-ray (EDX)

The examination was conducted using EDX to reveal the purity of the silver formed and the nature of the elements accompanying the nanomaterial [17].

2-5-7 : The effect of AgNPs on the growth of pathogenic bacteria

Pathological isolates isolated from acute infections (*Pseudomonas aeruginosa*, *E. coli*, *Klebsiella pneumonia*, and *Staphylococcus aureus*) were cultured, and the Well diffusion method was used to detect the diameters of inhibition of silver nanoparticles, where four concentrations were used (25, 50, 75, and 100 µg/ml). The bacterial species were grown on Muller-Hinton agar medium, holes with a diameter of 6 mm were made, and 200 µl of nanosilver concentrate was added to the holes [18].

2-5-8 : Determine the minimum inhibitory concentration.

Test tubes were produced, each containing 1.8 ml of nutrient broth medium. For each bacterial species (Pseudomonas aeruginosa, E. coli, Klebsiella pneumonia, Staphylococcus aureus), a bacterial suspension was introduced to the tubes. Additionally, nanosilver concentrations were also added to the tubes. Control tubes were prepared by combining the bacterial suspension with the nutritional medium, without the addition of silver nanoparticles. Subsequently, all tubes were placed in the

incubator and incubated at a temperature of 37 °C for a duration of 24 hours. Following the completion of the incubation time, the level of cloudiness in the control tubes was compared to the tubes that included both the bacterial cultures and silver nanoparticles. By monitoring the lowest level of cloudiness present in the tubes, the minimum inhibitory concentration was established [19].

2-5-9 : The effect of silver nanoparticles on catalase enzyme production in pathogenic bacteria

Eight test tubes containing 1.8 ml of nutrient broth medium were prepared, and the bacterial suspension for the pathogenic isolates was added to them. The minimum inhibitory concentration was added to four tubes containing the bacterial cultures, and four containers were left on the bacterial cultures without adding silver nanoparticles, and they were considered control factor The tubes were incubated in the incubator at a temperature of 37 °C for 24 hours, and after the end of the incubation period, a few drops of treated and untreated bacterial cultures were taken and placed on the surface of a glass slide, and drops of a 3% hydrogen peroxide solution were added to it. It was observed that bubbles appeared or did not appear. Its appearance is [20].

2-5-10 : Inhibition of biofilm formation by silver nanoparticles

Test tubes containing 5 ml of nutrient broth medium were prepared, and 1 ml of 2% glucose solution was added to them. The bacterial suspension of pathogenic bacterial species was added to the test tubes and mixed well using a vortex device. 0.1 ml of nutrient broth medium was added to the pits of a plate. The calibration was considered a negative control factor, and bacterial cultures were added to the remaining pits in an amount of 0.1 ml and were considered a control factor Positively, an ELISA device was used, and the absorbance of the positive control pits was compared with the negative control pits according to Table 1, where (A) refers to the positive control pit and (AC) refers to the negative control pit. The effectiveness of silver nanoparticles against film formation was measured. Biotechnology by means of where 0.1 ml of bacterial cultures of the four species were added to the pits and it was considered a negative control factor, and 0.08 ml of bacterial cultures were added to the remaining pits and nanosilver concentrations (0.02) were added (25, 50, 75, 100 µg\ ml) and was considered a positive control factor, as the microtiter plate was incubated at a temperature of 37 °C. For 24 hours, after the end of the incubation period, the contents of the plate were emptied and washed with a PBS solution. The plate was left to dry at room temperature for 10 minutes, then the crystal violet dye was added and left for 5 minutes. After that, the contents of the plate were emptied and washed with a PBS solution. Added to it was glacial acetic acid at a concentration of 33%. The intensity of biofilm formation and the inhibition power of AgNPs were measured using an ELISA device [21]. The inhibition power of silver nanoparticles on biofilm formation was calculated according to the inhibition equation [22].

Table 1 Shows the Intensity of biofilm formation in pathogenic isolates

$A \leq AC$	Non-biofilm forming
$AC \leq A \leq 2 * AC$	Medium biofilms
$2 * AC \leq A$	Strong biofilms

$$\text{Inhibition of biofilm} = \frac{\text{Negative control wavelength} - \text{positive control Wavelength}}{\text{Negative control wavelength}} \times 100$$

The equation for calculating the biofilm inhibition percentage

Result and Discussion

3-1 : Sample collection

E. coli bacteria were isolated from soil taken from the edge of the Euphrates River in the northern Basra city. The soil sample was diluted with distilled water and spread on nutrient agar medium. The isolate was purified based on its phenotypic and microscopic characteristics and molecular diagnosis.

3-2 : Appearance characteristics

Colonies of *E. coli* bacteria appeared pink in color, solid and dry in consistency, and medium size

when grown on MacConky agar medium due to their ability to ferment the sugar lactose, as in Figure 1 [23]. When grown on blood agar medium, the bacteria showed the ability to decompose blood. The β type possesses the enzyme hemolysin [24].

3-3 : Microscopic diagnosis

After staining with Gram stain and examining it under microscopy it appeared that the cells were single rod-shaped or clustered in pairs and did not form spores, as in Figure 1 [25].

Figure 1: Growth of *E. coli* bacteria on MacConky agar medium and fermentation of lactose

3-4 : Biochemical tests

E. coli bacteria showed positive results for many tests and negative results for some, as shown in Table 2.

Table 2: Results of biochemical tests for *E. coli* bacteria

Isolate	Indole	MRD	Catalase	Oxidase	Citrate	Urease
E.coli	+	+	+	+	-	+

3-5 : Molecular diagnostics

A molecular diagnostic test was conducted for *E. coli* bacteria by using the *16S rRNA* gene to confirm the results of the phenotypic and microscopic examination. DNA was extracted from the bacteria, and the electrophoresis results showed the appearance of DNA bands on the agarose gel. When the bacterial DNA was amplified using the polymerase chain reaction (PCR), the chain reaction using primers (F27) and (R1492) showed that the size of the base pairs was 1492 bp when compared with the DNA ladder, as shown in Figure 2.. The technique was used Sanker performed a sequencing analysis of the resulting amplification of the *16S rRNA* gene, where the results showed a 99.87% match with the reference sample *E. coli* in GenBank with serial number MF919600.1, and the sample of the current study was registered in GenBank with number PP475417, as in Table 3.

Table 3: Percentage of identity with the reference sample in GenBank, the serial number of the reference sample, and the serial number of *E. coli* bacteria registered in GenBank

Identity %	Accession No.	GenBank sample	Accession NO.	Present sample
99.87 %	MF919600.1	*E.coli*	PP475416	*Escherichia coli*

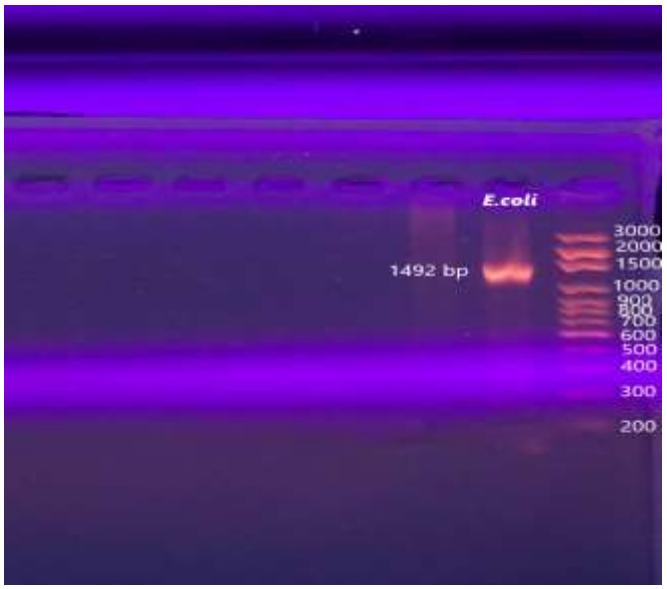

Figure 2: DNA amplification of *E. coli* bacteria compared to the DNA ladder

3-6 : Characterization of AgNPs

3-6-1: Change in color

The reaction mixture consisting of 90 ml of the supernatant solution of *E. coli* bacteria with 10 ml of AgNO3 solution at a concentration of 1 mM showed that the color of the reaction mixture changed from yellow to brown, which indicates the reduction of silver nitrate salts to silver nanoparticles [26]. As in Figure 3.. The reason why the reaction mixture does not appear silvery is due to the phenomenon of plasmon resonance that occurs in metals when the diameters of their particles reach nanoscale diameters (1–100 nm). [27]

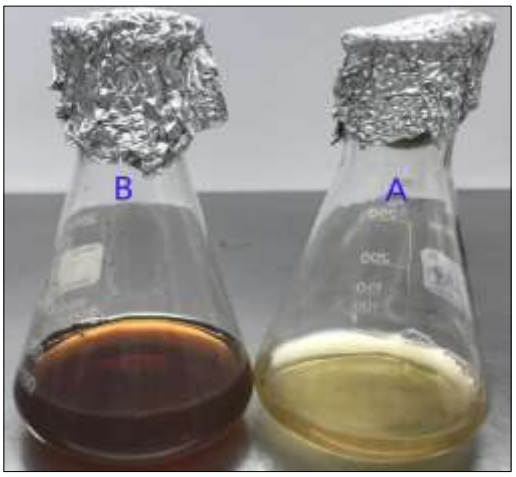

Figure 3: The bacterial supernatant was treated with 1 mM of AgNO3 before and after incubation for 24 h. The biosynthesis was confirmed by changing the color of the reaction as a visual indicator.

3-6-2 : : UV-visible spectroscopy

The results of the examination using UV-Vis spectrophotometer analysis showed the appearance of an absorption peak at the wavelength (428 nm), which is evidence of the formation of silver nanoparticles, as in Figure 4.. The results agreed with [28] in using the supernatant solution of *E. coli* bacteria in the reduction of silver nitrate salts.

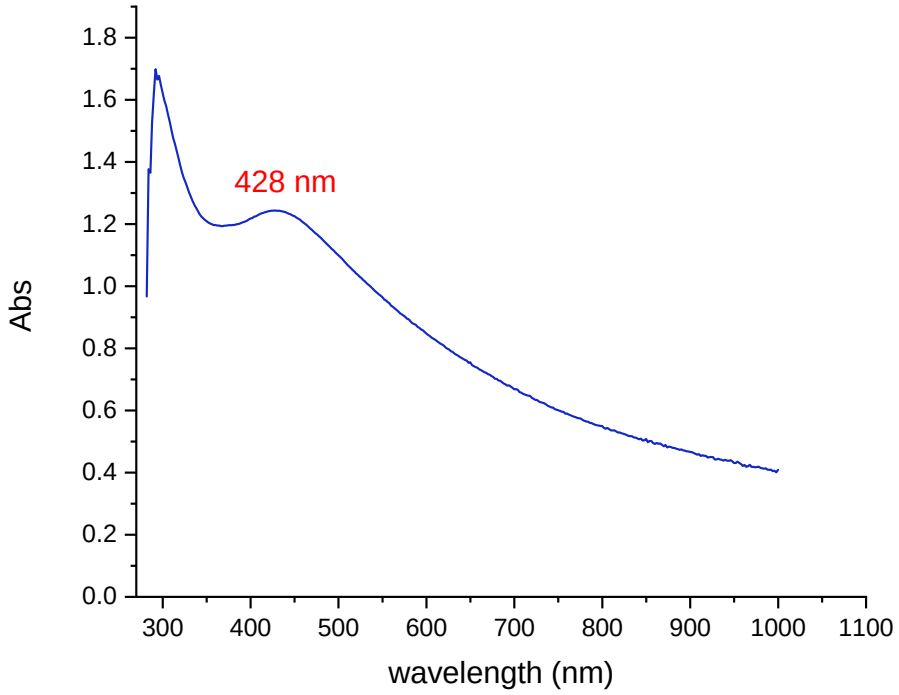

Figure 4 shows the UV-vis absorption curve of the reaction mixture after incubation. The maximum absorption peak of the surface plasmon of AgNPs is present at 428 nm.

3-6-3 : Fourier-transform infrared spectroscopy (FT-IR)

The FT-IR examination showed the appearance of many active groups that contributed to the reduction of AgNO3 silver nitrate salts into silver nanoparticles. The infrared device showed the appearance of different peaks for the active groups, as a peak appeared at 3305.39 $^{cm-1}$, which expresses the N-H bond present in the aliphatic primary amine group, and another peak appeared at 2360.44 $^{cm-1}$, which indicates the O=C=O bond present in the carbon dioxide group, while the peak at 1643.05 $^{cm-1}$ indicated the presence of the C=C is located in the alkene group

A peak appeared at 663.393 ^{cm1}, indicating the presence of the C-Cl bond present in the group of halo compounds, as shown in Figure 5.. These compounds contributed to the reduction of silver nitrate salts and their conversion into silver nanoparticles, in addition to their role in encapsulating AgNPs and preventing the oxidation process of these particles [29].

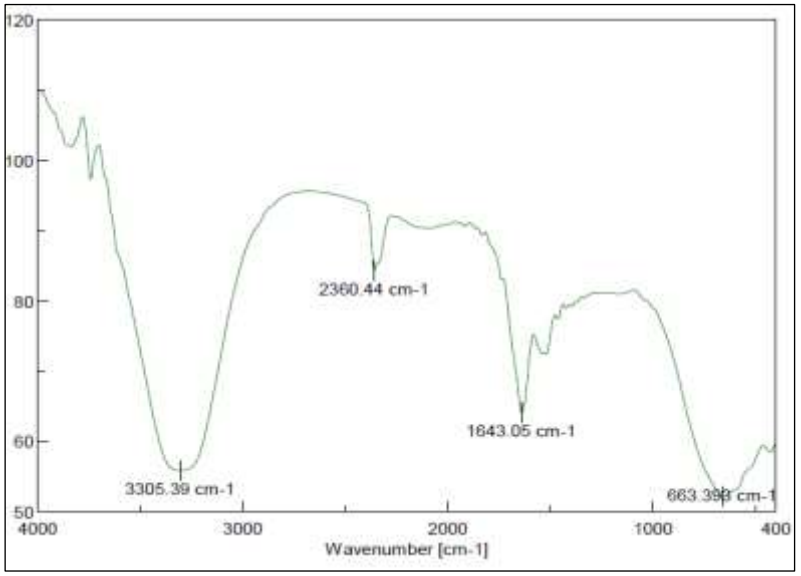

Figure 5 FT-IR of silver nanoparticles formed by *E. coli* supernatant. The spectrum of FTIR identified the unique peaks at 3305.39 $^{cm-1}$, 2360.44 $^{cm-1}$, 1643.05 $^{cm-1,}$ and 663.393 $^{cm-1.}$

3-6-4 : Examination using SEM and TEM

The SEM results showed that the nanoparticles formed had spherical shapes and sizes ranging between 11.68 and 47.66 nm and an average of 23.88 nm. The TEM results confirmed that the nanoparticles appeared in a spherical shape that prevailed among the particles and that the sizes ranged between 13.17 and 40.01 nm at a rate of 27.57 nm, as shown in Figure 6.. The results of the current study agree with [30].

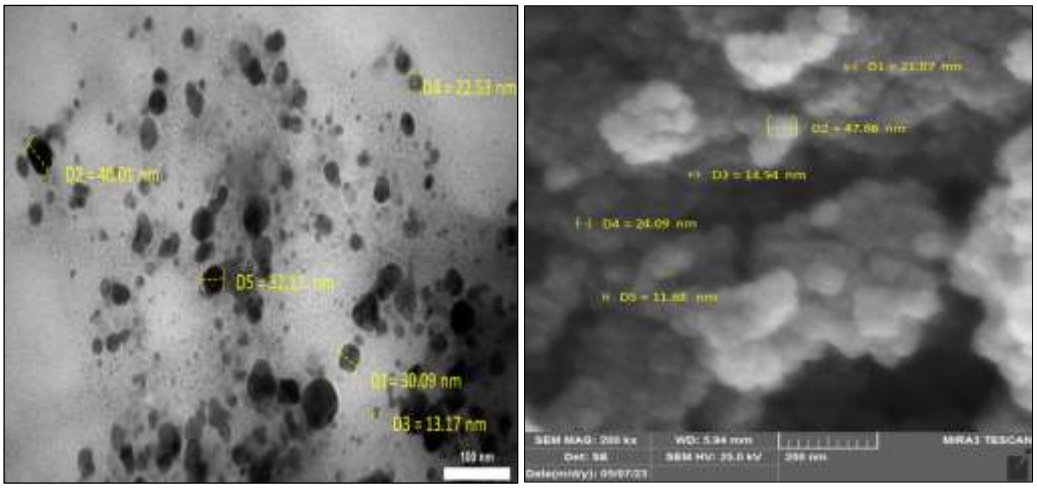

Figure 6 TEM and SEM Pictures of AgNPs synthesized by *E. coli* (A) SEM and (B) TEM show an aspherical shape. The average size in TEM was 27.57 nm, and in SEM it was 23.88 nm.

3-6-5 : X-ray diffraction (XRD)

An X-ray diffraction examination was conducted for silver nanoparticles synthesized using *E. coli* bacteria to detect the crystalline pattern of the formed particles. The silver particles were examined with an XRD device, and the data generated from the device was processed using the X'Pert HighScore program to obtain the crystalline form of nanosilver, the examination result showed the

appearance of peaks (111, 200, 220, 311) that corresponded to pool reflections from angles of 2Θ (38.11°, 44.27°, 64.42°, 77.47°), respectively, when compared with the JCPDS card. The same number (00-004-0783) is in the X-ray diffraction database. These results indicated the presence of silver nano Ag and its possession of a cubic crystal pattern (Cubic) .When examining the other peaks obtained, it was found that angles (26.65°, 32.79°, 47.07°, and 65.44°) appeared at the peaks (110, 111, 211, 220, 311) when compared with the JPCDS card number (00-041-1104). The results indicated the presence of silver nanoparticles with a cubic crystal pattern, as shown in Figure 7 [31].

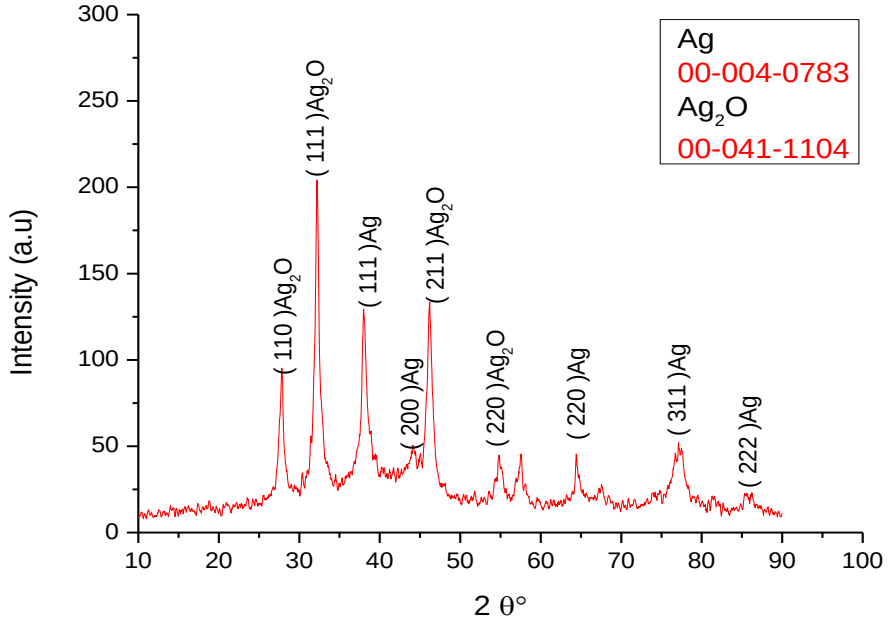

Figure 7 XRD of silver nanoparticles formed by *E. coli* supernatant. The XRD patterns at 2 θ values of 38.11 °, 44.27 °, 64.42 °, and 77.47 ° indicated the reflections of Ag, and 26.65 °, 32.79 °, 47.07 °, and 65.44 ° indicated the reflection of AgO

3-6-6 : Energy Dispersive X-ray Spectroscopy (EDX)

A test utilizing energy dispersive X-ray analysis was performed to identify the chemical composition of silver nanoparticles that were generated biologically by the extracellular manufacturing technique. The analysis revealed a significant concentration of silver, along with trace amounts of other metals. The EDX test findings revealed a prominent peak suggesting a significant presence of silver and a substantial overall quantity. The cumulative weight of the items featured in the test. Furthermore, a set of components was seen, including carbon, which is believed to be present due to its occurrence in the biomass and its existence in the bacteria's supernatant solution. The examination results indicated the presence of elements such as aluminum, magnesium, silicon, sodium, and nickel in small proportions relative to the total weight of the sample. These elements were found to be remnants from previous samples that had adhered to the silicon chip of the SEM device used for examination. Figure 8 displays the proportion of silver and other elements. The findings of the present investigation are consistent with the results reported in reference [32].

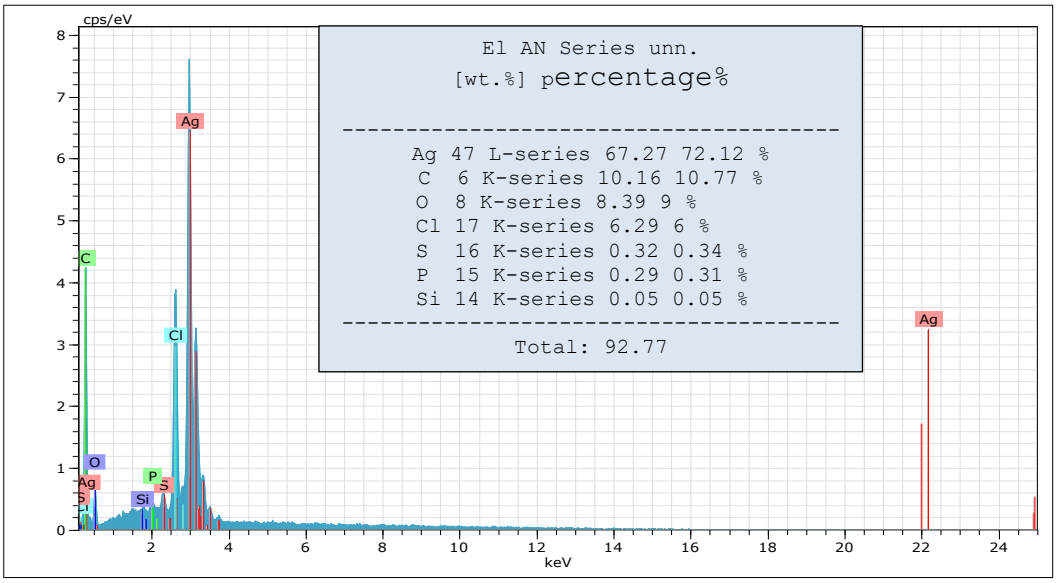

Figure 8 EDX analysis shows the percentage of formation of silver, carbon, oxygen, chlorine, silicon, phosphorus, and sulfur.

3-6-7 : Effect of silver nanoparticles on bacterial growth

The inhibitory ability of AgNPs on *P. aeruginosa*, *E. coli*, *K. pneumoniae*, and *S. aureus* bacteria was examined using the etch diffusion method, where silver nanoparticles synthesized from *E. coli* bacteria showed that they have the ability to inhibit bacterial growth when concentrations are used (25, 50, 75, 100 µg\ml), where the concentration (25 µg\ml) gave an inhibition diameter of (14.5, 14, 12, 15mm), while the concentration (50 µg\ml) gave diameters of inhibition (15, 15, 13, 18mm). On bacterial species, respectively, the concentration (75 µg\ml) gave diameters of inhibition (17, 16, 15, 19 mm), and the concentration (100 µg\ml) gave diameters of inhibition (18, 17, 16, 21mm) on the bacterial species. Respectively, the test results showed that AgNPs have the ability to inhibit the growth of pathogenic bacteria with different diameters of inhibition, as the diameters of inhibition increased at high concentrations, and the results showed a clear increase in the diameters of inhibition when concentrations increased. The results showed that there is a difference between the diameters of inhibition between the pathogenic bacterial isolates, which is attributed to the difference in the structure of the cell wall and the physiology of the bacterial cells, in addition to the cellular metabolism of the bacteria through the enzymes that the bacteria possess [33]. Figure 9 and Chart 1 show the inhibition diameters of silver nanoparticles, and the results of the current study were consistent with [34]

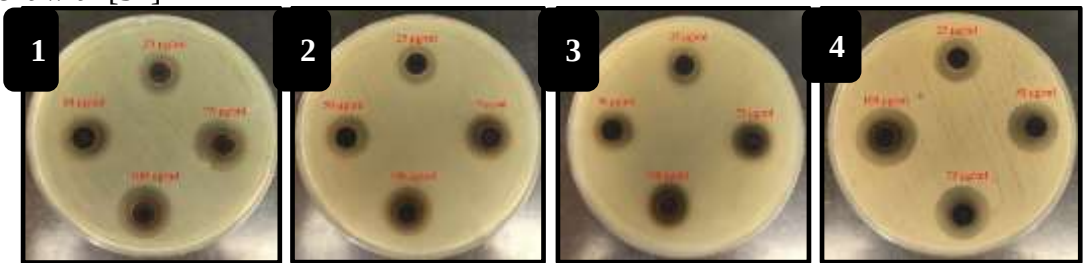

Figure 9 shows the diameters of inhibition on bacteria 1 (*P. aeruginosa*), 2 (*E. coli*), 3 (*K. pneumoniae*), and 4 (*S. aureus*) on Muller-Hinton agar medium using concentrations. (25 µg\ml , 50 µg\ml , 75 µg\ml , 100 µg\ml)

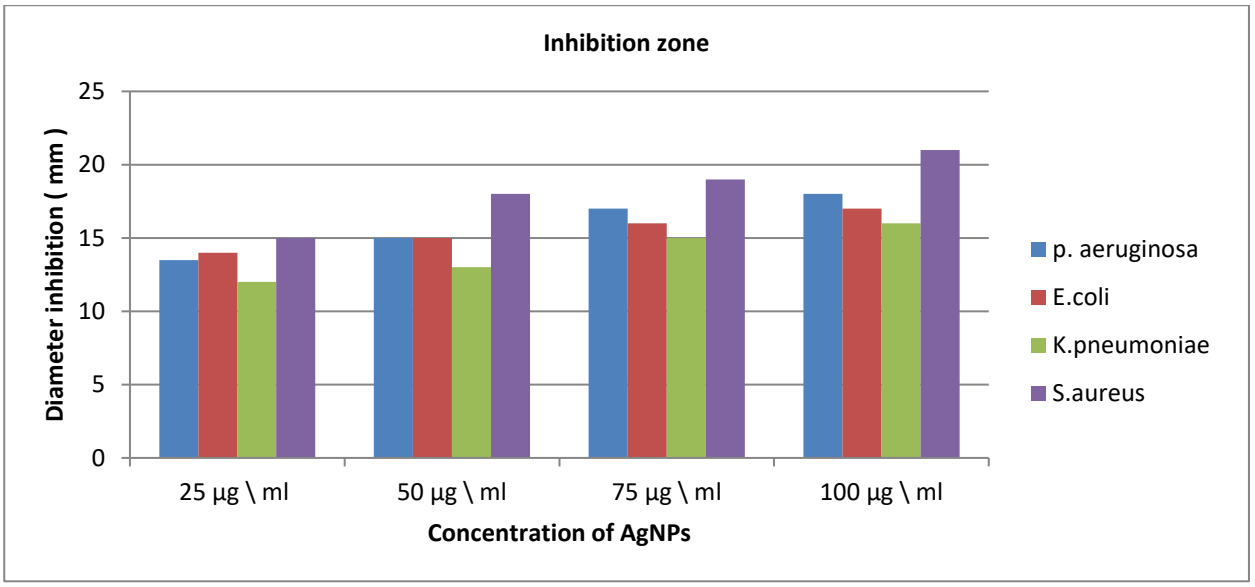

Chart 1 shows the percentages of inhibition on bacterial species when using AgNPs produced from *E. coli* bacteria.

3-6-8 : Determine the minimum inhibitory concentration.

The results showed that silver nanoparticles reached a minimum inhibitory concentration on bacterial species of about 25µg/ml, as in Table (4) and Figure (10). The thickness of the biofilm of bacterial cells plays an important role in determining the percentage of inhibitory concentration, as the passage of nanoparticles The throughput of the plasma membrane depends on the thickness of the plasma membrane [35].

Table 4 shows the minimum inhibitory concentration for the bacterial species *P. aeruginosa*, *E. coli*, *K. pneumoniae*, and *S. aureus*.

Minimum inhibitory concentration	Types of bacteria
25µg\ml	*P. aeruginosa*
25µg\ml	*E.coli*
25µg\ml	*K.pneumoniae*
25µg\ml	*S.aureus*

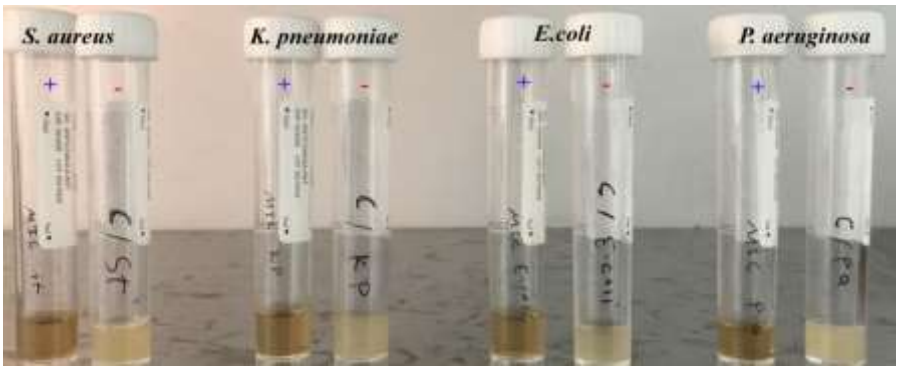

Figure 10 shows the percentage of turbidity in the negative control agent for bacterial cultures not treated with silver nanoparticles compared to the positive control agent containing bacterial cultures with silver nanoparticles to determine the minimum inhibitory concentration.

3-6-9 : The effect of silver nanoparticles on the production of the catalase enzyme

The test results showed that silver nanoparticles had the ability to inhibit catalase production in pathogenic bacterial isolates when a concentration of 25 µg/mL was used. The test results showed that bacterial cultures not treated with silver nanoparticles showed bubbles when hydrogen peroxide was added at a concentration of 3%, which is evidence of the production of the catalase enzyme, as the catalase enzyme is the most common enzyme in bacteria, as it works to decompose hydrogen peroxide into oxygen and water, while bacterial cultures treated with silver nanoparticles did not show bubbles when hydrogen peroxide was added, which tends to inhibit the production of the catalase enzyme, as in Figure (11). The results of the current study agree with [36].

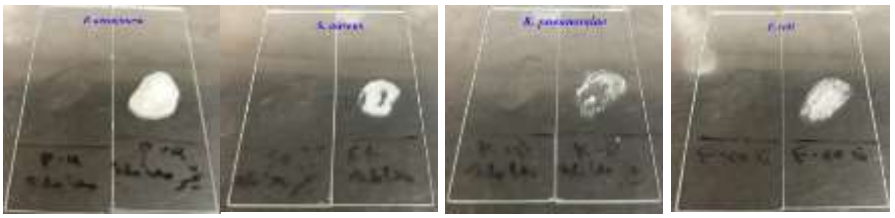

Figure (11) shows the production of catalase in bacterial cultures not treated with silver nanoparticles and bacterial cultures treated with silver nanoparticles in which catalase was not produced.

3-6-10 : Measuring the intensity of biofilm formation using a microtiter plate

The results of the ELISA device showed that when comparing the absorbance of the control pits AC containing the culture medium only with the pits containing the bacterial culture A, it was found that the biofilm formed in the bacterial isolates was of high intensity, as the pit containing the bacterial culture *P. aeruginosa* (A) showed Absorbance (1.098), while the absorbance of the control pit (AC) was (0.087), and the pit containing the bacterial culture *E. coli* (A) showed an absorbance of (1.433), while the absorbance of the control pit (AC) was (0.078), and the pit containing the bacterial culture showed *K. pneumonia* (A) absorbance (1.175), while the absorbance of the control hole (AC) was (0.097), and the examination showed the absorbance of the hole containing the *S. aureus* bacterial culture (A) (1.288), while the absorbance of the control hole (AC) was (0.098). Table 5 and Figure 12 show the intensity of biofilm formation in bacterial isolates, and the results agree with [37].

Table (5) shows the intensity of biofilm formation in pathogenic bacterial isolates. (AC) negative control pits containing the culture medium only. (A) control pits containing biofilm-forming bacterial cultures.

Biofilm response	Biofilm Formation		Isolates
strongly biofilm	2* 0.088 ≤ 1.098	2 * AC ≤ A	*P. aeruginosa*
strongly biofilm	2* 0.087 ≤ 1.433	2 * AC ≤ A	*E.coli*
strongly biofilm	2* 0.097 ≤ 1.175	2 * AC ≤ A	*K. pneumonia*
strongly biofilm	2* 0.098 ≤ 1.288	2 * AC ≤ A	*S. aureus*

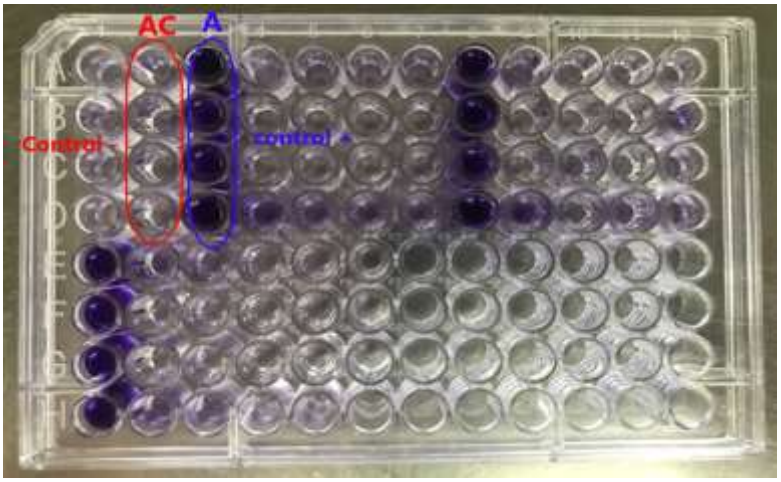

Figure (12) Microtiter plate containing the bacterial cultures forming the biofilm (AC), the negative control hole (A), and the positive control hole forming the biofilm

3-6-11 : Effect of silver nanoparticles against biofilm formation by microtiter plates

The effectiveness of silver nanoparticles formed by *E. coli* bacteria against biofilm formation was determined using a microtiter plate. The results showed, when applying the inhibition equation, that the highest rate of inhibition reached (92.27%) on *K. pneumonia* bacteria at a concentration of 100µg/ml, even if it was less. The inhibition rate reached 82.80% on *P. aeruginosa* bacteria at a concentration of 25 µg/ml,, as in Table (6) and Figure (13), and the results were consistent with [38].

Table 6: Biofilm inhibition rates in biofilm-forming bacterial isolates using silver nanoparticles using concentrations (25 µg/mL, 50 µg/mL, 75 µg/mL, and 100µ g/mL)

Nanosilver concentrations				Types of bacteria
100µg\ml	75µg\ml	50µg\ml	25µg\ml	
89.97	89.27	88.03	82.80	*P. aeruginosa*
91.93	90.50	89.40	87.43	*E.coli*
92.80	91.50	89.73	88.03	*K. pneumonia*
91.27	90.33	89.10	83.47	*S. aureus*

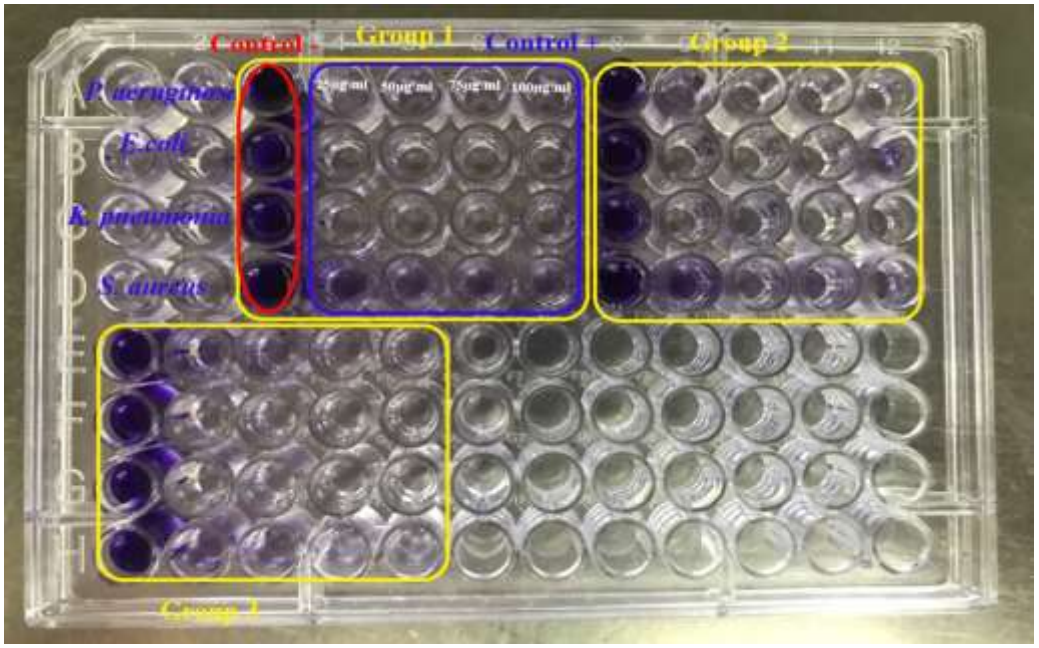

Figure 13 shows a microtiter plate containing cultures of biofilm-forming bacterial isolates and the rates of biofilm inhibition using silver nanoparticles formed by *E. coli*

References

[1]. Ahmed, T., Shahid, M., Noman, M., Niazi, M. B. K., Mahmood, F., Manzoor, I., ... & Chen, J. (2020). Silver nanoparticles synthesized by using Bacillus cereus SZT1 ameliorated the damage of bacterial leaf blight pathogen in rice. *Pathogens*, *9*(3), 160.

[2]. El-Shanshoury, A. E. R. R., ElSilk, S. E., & Ebeid, M. E. (2011). Extracellular biosynthesis of silver nanoparticles using *Escherichia coli* ATCC 8739, Ba-cillus subtilis ATCC 6633, and Streptococcus thermophilus ESh1 and their antimicrobial activities. *International Scholarly Research Notices*, *2011*.

[3]. - Syafiuddin, A. (2017). Salmiati; Salim, MR; Beng Hong Kueh, A.; Hadibarata, T.; Nur, H.

A review of silver nanoparticles: Research trends, global consumption, synthesis, properties, and future challenges. *J. Chin. Chem. Soc*, *64*(7), 732-756.

[4]. Villeret, B., Dieu, A., Straube, M., Solhonne, B., Miklavc, P., Hamadi, S., ... & Garcia-Verdugo, I. (2018). Silver nanoparticles impair retinoic acid-inducible gene I-mediated mitochondrial antiviral immunity by blocking the autophagic flux in lung epithelial cells. *ACS nano*, *12*(2), 1188-1202.

[5]. Schillaci, D., Cusimano, M. G., Cascioferro, S. M., Di Stefano, V., Arizza, V., Chiaramonte, M., ... & Venturella, G. (2017). Antibacterial activity of desert truffles from Saudi Arabia against Staphylococcus aureus and Pseudomonas aeruginosa. *International Journal of Medicinal Mushrooms*, *19*(2).

[6]. Stoodley, P., Sauer, K., Davies, D. G., & Costerton, J. W. (2002). Biofilms as complex differentiated communities. *Annual Reviews in Microbiology*, *56*(1), 187-209.
7-

[7]. Laxminarayan, R., Duse, A., Wattal, C., Zaidi, A. K., Wertheim, H. F., Sumpradit, N., ... & Cars, O. (2013). Antibiotic resistance—the need for global solutions. *The Lancet infectious diseases*, *13*(12), 1057-1098.

[8]. Johnson, L. F., Curl, E. A., Bond, J. H., & Fribourg, H. A. (1960). Methods for studying soil microflora-plant disease relationships.

[9]. Hashim, A. I. (2020). *Cytotoxic effects of silver nanoparticles prepared from Escherichia coli culture filtrates on vero cell line* (Doctoral dissertation, M. Sc. Thesis. Mustansiriyah University).

[10]. 10 - Nagati, V. B., Alwala, J., Koyyati, R., Donda, M. R., Banala, R., & Padigya, P. R. M. (2012). Green synthesis of plant-mediated silver nanoparticles using Withania somnifera leaf extract and evaluation of their antimicrobial activity. *Asian Pac J Trop Biomed*, *2*, 1-5.

[11]. Sathishkumar, M., Sneha, K., Won, S. W., Cho, C. W., Kim, S., & Yun, Y. S. (2009). Cinnamon zeylanicum bark extract and powder mediated green synthesis of nano-crystalline silver particles and its bactericidal activity. *Colloids and Surfaces B: Biointerfaces*, *73*(2), 332-338.

[12]. Al-Saady, O. M. F., & Zaki, N. H. (2022). THE EFFECT OF BIOSYNTHESIZED AG-NANOPARTICLES ON KLEBSIELLA PNEUMONIAE BIOFILM AND SOME VIRULENCE GENES. *CHINESE JOURNAL OF MEDICAL GENETICS*, *32*(4), 2022.

[13]. Sohrabnezhad, S. H., Moghaddam, M. M., & Salavatiyan, T. (2014). Synthesis and characterization of CuO–montmorillonite nanocomposite by thermal decomposition method and antibacterial activity of nanocomposite. *Spectrochimica Acta Part A: Molecular and Biomolecular Spectroscopy*, *125*, 73-78.

[14]. Hussain, Z. (2016). *Inhibition of Biofilm using biological synthesis of silver nanoparticles from supernatants of E. coli* (Doctoral dissertation, M. Sc. Thesis. Mustansiriyah University).

[15]. Hashim, A. I. (2020). *Cytotoxic effects of silver nanoparticles prepared from Escherichia coli culture filtrates on vero cell line* (Doctoral dissertation, M. Sc. Thesis. Mustansiriyah University).

[16]. Ramalingam, V: Rajaraml 1, R.: Premkumar, C.; Santhanam, -P.; Vinothkumar, s and Kaleshkumar, k. (2013). Dhi Biosnthesis of silver nanoparticles from deep sea bacteria Pseudomonas *aeruginosa*.

[17]. Neethu, S., Midhun, S. J., Sunil, M. A., Soumya, S., Radhakrishnan, E. K., & Jyothis, M. (2018). Efficient visible light induced synthesis of silver nanoparticles by Penicillium polonicum ARA 10 isolated from Chetomorpha antennina and its antibacterial efficacy against Salmonella enterica serovar Typhimurium. *Journal of Photochemistry and Photobiology B: Biology*, *180*, 175-185.

[18]. bakht Dalir, S. J., Djahaniani, H., Nabati, F., & Hekmati, M. (2020). Characterization and the evaluation of antimicrobial activities of silver nanoparticles biosynthesized from Carya illinoinensis leaf extract. *Heliyon*, *6*(3).

[19]. Ahmad, A., Wei, Y., Syed, F., Tahir, K., Rehman, A. U., Khan, A., ... & Yuan, Q. (2017). The effects of bacteria-nanoparticles interface on the antibacterial activity of green synthesized silver nanoparticles. *Microbial pathogenesis*, *102*, 133-142.
[20]. Patil, S. V., Borase, H. P., Patil, C. D., & Salunke, B. K. (2012). Biosynthesis of silver nanoparticles using latex from few euphorbian plants and their antimicrobial potential. *Applied biochemistry and biotechnology*, *167*, 776-790.
[21]. Ali, O. A. U. (2012). Prevention of Proteus mirabilis biofilm by surfactant solution. *Egyptian Academic Journal of Biological Sciences, G. Microbiology*, *4*(1), 1-8.
[22]. Namasivayam, S. K. R., Preethi, M., Bharani, A., Robin, G., & Latha, B. (2012). Biofilm inhibitory effect of silver nanoparticles coated catheter against Staphylococcus aureus and evaluation of its synergistic effects with antibiotics. *Int J Biol Pharm Res*, *3*(2), 259-265.
[23]. Wanger, A., Chavez, V., Huang, R., Wahed, A., Dasgupta, A., & Actor, J. K. (2017). Microbiology and molecular diagnosis in pathology: a comprehensive review for board preparation, certification and clinical practice.
[24]. MacFaddin, J. F. (2000). Biochemical tests for identification of medical bacteria, williams and wilkins. *Philadelphia, PA*, *113*(7).
[25]. Benson, H. J. (2002). *Microbiological applications: a laboratory manual in general microbiology*. [McGraw-Hill].
[26]. Zaki, N. H., & Husain, Z. (2016). Enhanced antibacterial and anti-biofilm activities of biosynthesized silver nanoparticles against pathogenic bacteria. *J Genetic Environ Res Conservation*, *4*(2), 197-203.
[27]. Saravanan, M., Barik, S. K., MubarakAli, D., Prakash, P., & Pugazhendhi, A. (2018). Synthesis of silver nanoparticles from Bacillus brevis (NCIM 2533) and their antibacterial activity against pathogenic bacteria. *Microbial pathogenesis*, *116*, 221-226.
[28]. Kathiresan, K., Alikunhi, N. M., Pathmanaban, S., Nabikhan, A., & Kandasamy, S. (2010). Analysis of antimicrobial silver nanoparticles synthesized by coastal strains of Escherichia coli and Aspergillus niger. *Canadian Journal of Microbiology*, *56*(12), 1050-1059.
[29]. Majeed, S., Aripin, F. H. B., Shoeb, N. S. B., Danish, M., Ibrahim, M. M., & Hashim, R. (2019). Bioengineered silver nanoparticles capped with bovine serum albumin and its anticancer and apoptotic activity against breast, bone and intestinal colon cancer cell lines. *Materials Science and Engineering: C*, *102*, 254-263.
[30]. Kathiresan, K., Alikunhi, N. M., Pathmanaban, S., Nabikhan, A., & Kandasamy, S. (2010). Analysis of antimicrobial silver nanoparticles synthesized by coastal strains of Escherichia coli and Aspergillus niger. *Canadian Journal of Microbiology*, *56*(12), 1050-1059.
[31]. Mbagwu, F. O., Auta, S. H., Bankole, M. T., Kovo, A. S., & Abioye, O. P. (2023). Biosynthesis and characterization of silver nanoparticles using Bacillus subtilis, Escherichia coli, and leaf extracts of Jatropha and Ocimum species. *International Nano Letters*, *13*(1), 63-73.
[32]. Huq, M. A. (2020). Green synthesis of silver nanoparticles using Pseudoduganella eburnea MAHUQ-39 and their antimicrobial mechanisms investigation against drug resistant human pathogens. *International journal of molecular sciences*, *21*(4), 1510.
[33]. Shareef, H. A., Jafar, N. B., & Abdulrahman, R. B. (2019). The Biosynthesis of Silver Nanoparticles by Moringa Oleifera and its Antibacterial Activity. *Indian Journal of Public Health Research & Development*, *10*(8).
[34]. Neihaya, H. Z., & Zaman, H. H. (2018). Investigating the effect of biosynthesized silver nanoparticles as antibiofilm on bacterial clinical isolates. *Microbial pathogenesis*, *116*, 200-208.
[35]. Qader, Q. A., Noumi, B. S., & Saleh, R. F. (2021). Antibacterial effect of biosynthesis silver nanoparticles on Pseudomonas aeruginosa. *Tikrit Journal of Pure Science*, *26*(5), 22-26.
[36]. Hamida, R. S., Ali, M. A., Goda, D. A., Khalil, M. I., & Al-Zaban, M. I. (2020). Novel biogenic silver nanoparticle-induced reactive oxygen species inhibit the biofilm formation and

virulence activities of methicillin-resistant Staphylococcus aureus (MRSA) strain. *Frontiers in bioengineering and biotechnology*, *8*, 433.

[37]. 37- Kunwar, A., Shrestha, P., Shrestha, S., Thapa, S., Shrestha, S., & Amatya, N. M. (2021). Detection of biofilm formation among Pseudomonas aeruginosa isolated from burn patients. *Burns Open*, *5*(3), 125-129.

[38]. 38 - Siddique, M. H., Aslam, B., Imran, M., Ashraf, A., Nadeem, H., Hayat, S., ... & Muzammil, S. (2020). Effect of silver nanoparticles on biofilm formation and EPS production of multidrug-resistant Klebsiella pneumoniae. *Biomed research international*, *2020*(1), 6398165.